EXPERIMENTAL AND NUMERICAL COMPARISONS OF THE AEROACOUSTICS IN A CORRUGATED PIPE FLOW

Gaëtan Galeron, Pierre-Olivier Mattei, Muriel Amielh, Fabien Anselmet, Daniel Mazzoni

EXPERIMENTAL AND NUMERICAL COMPARISONS OF THE AEROACOUSTICS IN A CORRUGATED PIPE FLOW

Gaëtan Galeron
Pierre-Olivier Mattei
CNRS - UPR 7051, F-13453,
Marseille, France
galeron@irphe.univ-mrs.fr

Muriel Amielh
Daniel Mazzoni
Fabien Anselmet
Aix Marseille Université, CNRS, Centrale
Marseille, IRPHE UMR 7342,
Marseille, France

ABSTRACT

Our study is focused on the singing risers phenomenon which is encountered in corrugated channels under flow. Internal corrugations are responsible for flow instabilities that synchronize with longitudinal acoustic modes of the channel giving powerful pure tones.

Experiments are performed in a specifically designed facility. Numerical simulations of the flow based on a lattice Boltzmann method (LBM) are faced to the experimental results. They aimed at investigating the ability of a LBM based simulation to predict the aeroacoustics of corrugated channels.

Acoustic modes and turbulence in the corrugated channel are quite well predicted except the sound pressure levels that need better description of the acoustic boundary conditions at the open ends.

NOMENCLATURE

$\boldsymbol{x}$: position vector
t: time
$\{\xi_i\}_{i=0..8}$: velocity in the discrete velocity space
$\{f_i\}_{i=0..8}$: discrete probability density function in the discrete velocity space
f_i^{EQ}: discrete probability density function in absence of any collision
ρ: mass density
τ : relaxation time related to fluid viscosity
w_i: Gauss integration points
u: local resultant velocity vector
Δt: time step
c_{LB}: lattice constant
Δx: lattice discrete size
ν: kinematic viscosity of the fluid
c_s: speed of sound in air
P: pressure
$\boldsymbol{e_i}$: unit vector pointing in the direction of the discrete velocity space
$\Delta x_{mesh\ finest}$: finest mesh size
Δx_{mesh}: mesh size
U_0: time and spatial average mean velocity magnitude
f_n: Eigen frequencies
c_{eff}: effective speed of sound
L_p^*: theoretical sound pressure level
P_M^2: acoustic wave amplitude measured
n: n-th mode under consideration
δL: correction length of the channel.
$\tilde{u}$: time averaged mean velocity.

INTRODUCTION

Due to their flexibility and local stiffness, corrugated pipes are used in many engineering applications. In particular, they are widely used for the transport of natural gas. Under certain conditions of geometries and flow, the pipes may whistle, generating harmful vibrations to the adjoining industrial facilities. Our study is focused on this singing risers phenomenon that is encountered in corrugated pipes under flow. Internal corrugations are responsible for flow instabilities that may synchronize with longitudinal acoustic modes of the pipe giving powerful pure tones internal noise [1, 2, 3]. The turbulence of the flow, the interaction between the vortices developing inside the cavities forming the corrugation and finally the feedback whistling are to be studied to understand this aeroacoustic phenomenon [4, 5, 6]. Both laboratory experiments and numerical simulations are here proposed to this aim.

In our studies, the length of the pipe is large with respect to the dimensions of the cavities. The flow at the center of the pipe remains subsonic with velocities corresponding to a Mach number of less than 0.1. A short description of the especially designed laboratory facility is given. Simulations with the Lattice Boltzmann method (LBM) are faced to experimental results obtained for different flow configurations. Comparisons between experiments and calculations concern velocity and pressure. They aim at

investigating the ability of a LBM based simulation to predict the aeroacoustics of corrugated channels.

This paper aims at presenting two sets of calculations as we want to model our experimental facility. In the first set, a corrugated channel only has been modeled while in the second set upstream and downstream chambers have been added to the corrugated channel in order to better represent acoustics. Comparisons of these two sets of calculations will be presented forward.

EXPERIMENTAL SET-UP

The experimental facility under study is made of a low speed wind tunnel whose fan rotation speed ensures a flow velocity up to *25 ms*$^{-1}$. The tunnel is connected to a corrugated rectangular channel of length *L = 2 m* made of Plexiglas plates. The corrugated channel has lateral width *D = 20mm* and height *B = 100mm*. The lateral plates are machined in order to make a wall with a rectangular corrugation of pitch length *Pt = 20mm* that is repeated all along the channel.

The corrugation occupies the full height of the lateral walls of the channel. As shown in Figure 1, the corrugations are rectangular with a depth *H = 10mm*, and a width *w = 10mm*; the upstream corner of the corrugation is rounded with a curve with curvature radius *r = 2.5mm*. The top and bottom walls of the channel are perfectly smooth. The corrugations occupy about 83% of the wall surface of the channel.

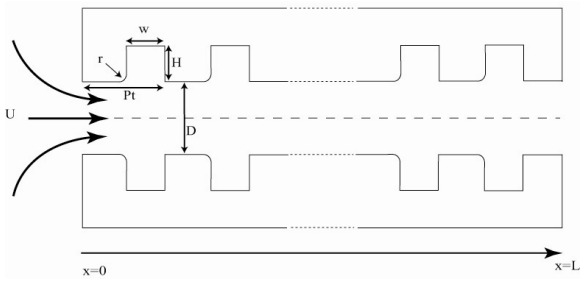

(a)

(b)

Figure 1 – Geometry of the corrugated channel. a) Schematic view, b) Photography of details of the face to face vertical corrugated plates.

Thanks to the transparency of the channel, optical techniques (Particle Image Velocimetry and high frequency visualization) are implemented in order to investigate in detail the flow field in the corrugation vicinity. Moreover, standard hot-wire anemometry and acoustic pressure measurements with microphones are performed.

LATTICE BOLTZMANN METHOD

Our numerical simulations use the Lattice Boltzmann Method (LBM) to predict the noise emission from the corrugated channel flow. The Lattice Boltzmann method differs from traditional patterns by numerically solving an equation based on the physical statistics. Given the limitation Mach number of the LBM, the main interest of the remaining compressibility is to bring the acoustic phenomena. The LBM ability to simulate the propagation of acoustic waves is presented in [7]. Recent developments of the LBM acoustic behavior are proposed in [8].

Although it is limited to weakly compressible flows, this method is efficient for predicting unsteady and compressible flows; thereby it can be used to simulate the acoustic waves in a turbulent flow [9]. In the present study, we use the EXA software 'PowerFlow'.

The Lattice Boltzmann Method is based on the kinetic theory for a fluid flow and from the Boltzmann Transport Equation from the classical kinetic theory of gases.

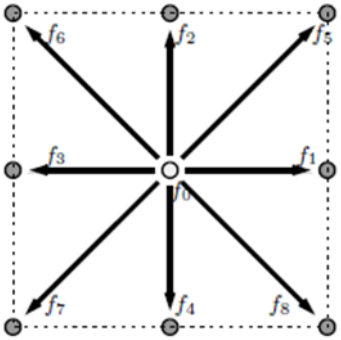

Figure 2 – Discrete probability density function with respect to the nine possible velocities for the particles in the D2Q9 case.

The discrete Boltzmann equation with the Bhatnagar-Gross-Krook (BGK) approximation [10] governs the evolution of the probability density function $f_i(\boldsymbol{x}, t) = f(\boldsymbol{x}, \xi_i, t)$ (i $= 0, \ldots, 8$) (see eq. 1). For the two dimensional nine velocities lattice (D2Q9, figure 2) used in the present study, ξ_i (i $= 0, \ldots, 8$) are the nine possible velocities for the particles in this discrete velocity space of finding a particle at the point **x**, at the date t, in absence of external forces.

$$\frac{\partial f_i}{\partial t} + \xi_i . \nabla f_i = -\frac{1}{\tau}(f_i - f_i^{EQ}) \qquad (1)$$

where f_i^{EQ} is the discrete probability density function in absence of any collision, f_i^{EQ} is usually taken as the second

order expansion of the Maxwell velocity distribution leading to:

$$f_i^{EQ}(\rho,u) = w_i\rho\left(1+\frac{\xi_i.u}{c_{LB}^2}+\frac{(\xi_i.u)^2}{2c_{LB}^4}-\frac{u^2}{2c_{LB}^2}\right) \quad (2)$$

where u is the local resultant velocity vector. $w_0 = \frac{4}{9}, w_{1,\dots,4} = \frac{1}{9}, w_{5,\dots,9} = \frac{1}{36}$ are the corresponding Gauss integration points to the ξ_i. $c_{LB} = \frac{1}{\sqrt{3}}$ is the lattice constant. τ is the relaxation time related to fluid viscosity, see eq. 6. The macroscopic fluid density and velocity are the moments of the discrete density function f_i:
Mass density:

$$\rho = \sum_i f_i = \sum_i f_i^{EQ} \quad (3)$$

Momentum flux:

$$\rho u = \sum_i \xi_i f_i = \sum_i \xi_i f_i^{EQ} \quad (4)$$

Integrating the Boltzmann equation (1) along the characteristics ξ_i, for a space-step equal to one ($\Delta x = 1$), denoting $\boldsymbol{e_i}$ the unit vector pointing in the direction of the velocity vector ξ_i, and supposing that the particles move from one cell per time step Δt (ie $\boldsymbol{\Delta x\, e_i} = \Delta t\, \xi_i$), one obtains the Lattice Boltzmann Equation (LBE):

$$f_i(\boldsymbol{x}+\boldsymbol{e_i}, t+\Delta t) - f_i(\boldsymbol{x},t) = -\frac{\Delta t}{\tau}\left(f_i(\boldsymbol{x},t) - f_i^{EQ}(\boldsymbol{x},t)\right) \quad (5)$$

Chapman-Enskog analysis [11] shows that in the limit of long-wavelengths, low-frequency, the LBE reproduces exactly the Navier-Stokes equation for weakly compressible flows with an ideal equation of state that is: $P = \rho c_s^2$ where P is the pressure and where $c_s = 343\, ms^{-1}$ is the speed of sound in air. The kinematic viscosity of the fluid ν is:

$$\nu = c_s^2\left(\tau - \frac{\Delta t}{2}\right) \quad (6)$$

NUMERICAL SET-UP

As first simulations, we represented a 2D corrugated channel alone. As regards the boundary conditions, we assigned a uniform velocity at the inlet and a pressure at the outlet.

Two predictable and an unexpected problems have been encountered. First one was the veina contracta phenomenon that was missing numerically and that appears to be determinant on our experimental facility. Second one was a bad representation of the acoustic boundary conditions (Neumann-Dirichlet) which differs from the Dirichlet-Dirichlet conditions found experimentally. Last one was a bad modeling of turbulence.

As a consequence, we decided to run a second set of calculations. Downstream and upstream chambers have been added to the corrugated channel. The upstream one has been added to solve the first two issues whereas the downstream one has been added to solve the last issue. In fact, we are expecting the acoustic to radiate outside the channel with the downstream chamber presence. As a result, turbulence could be better represented since acoustics would be less dominant.

Acoustic modes and flow shape in the corrugated channel were quite well predicted by the first calculations, except for the sound pressure levels and turbulence that need better description of the boundary conditions. Conditions of whistling appearance were also not well predicted so far.

These first results lead us to extend the calculation domain. We modeled a major part of the blowing wind tunnel upstream the corrugated channel The role of the upstream tranquillizer chamber is to introduce a sudden change of section of the flow path leading firstly to the flow destabilization and secondly to an approximated Dirichlet acoustic boundary condition. Downstream conditions consist in a large chamber at atmospheric pressure level. In order to attenuate the acoustic waves propagating in the chambers, the use of damping zones is compulsory. Those consist in various zones in which the viscosity increases as the waves move away from the corrugated pipe extremities. Four viscosity levels are introduced (Figure 3).

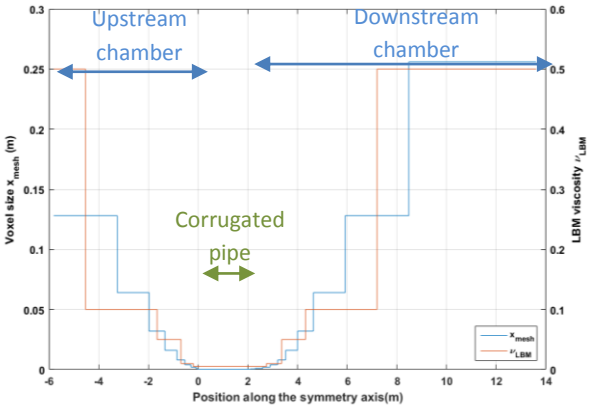

Figure 3 – Parameters for the second set of calculations.

As well as the viscosity increases, the voxel size increases. One can obtain the following curve which represents viscosity and voxel size along the symmetry axis of the corrugated pipe (Figure 3).

The finest voxel size is prescribed putting 100 points along the characteristic length $r + w = 12.5\, mm$ which lead to $\Delta x_{mesh\ finest} = 1.25\, 10^{-4}\, m$. Eleven levels of discretization are defined which impose 0.25m as the coarsest voxel size since between two levels, voxel size is doubled.

As a result, a 20 meters by 24 meters simulation area has been modeled (Figure 4 (a)). The geometry is a 2m long and 20mm wide two-dimensional channel with corrugated walls (Figure 4 (b)). The wall-cavities are identical to the experiment. At the inlet of the domain, a uniform velocity profile is used. At the outlet, a constant pressure condition is imposed that insures acoustic Dirichlet boundary conditions.

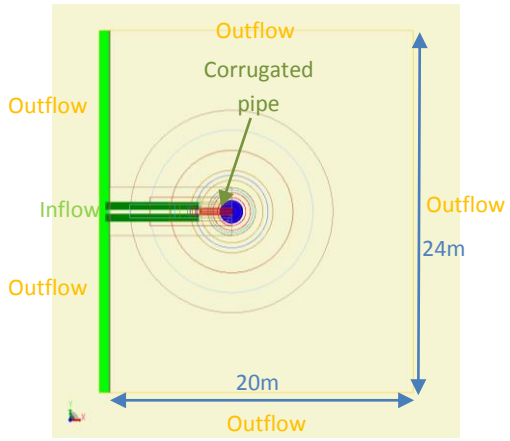

(a)

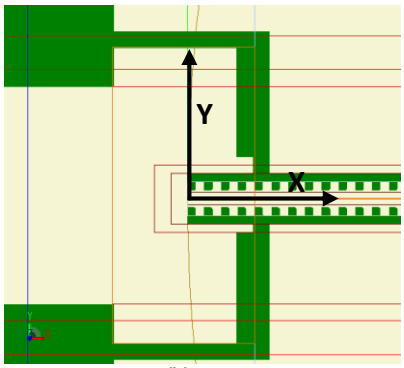

(b)

Figure 4 – Calculation domain for the second set of calculations. (a) Whole domain. (b).Zoom at the corrugated pipe inlet.

As initialization, a coarse simulation has been run. This consists in erasing the two finest grid levels of the simulation. Since the number of time steps to perform a 1 second of physical time simulation is proportional to the finest voxel size, this choice reduces consequently the computational time to simulate 1 second of physical time. The coarse simulation result has been chosen to initialize the wished fine simulation.

The first calculations were launched on 24 processors on the IRPHÉ cluster, as 3.867.200 voxels were used. Simulation was run for 1-second physical time that represented 4.893.808 time steps. The most recent calculations were run on 32 or 48 processors. For these simulations, 4.892.368 voxels were used.

RESULTS

The comparison of the numerical results with the experimental ones may lead to validate the computational study in order to perform further numerical investigations.

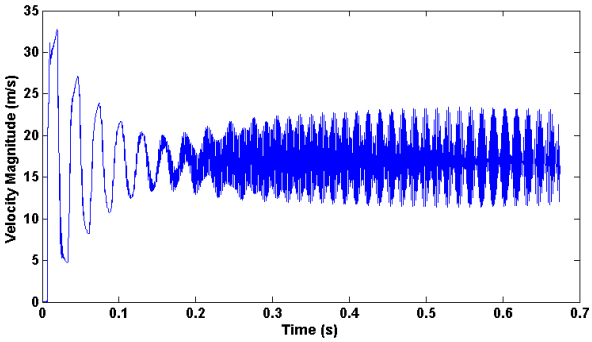

(a)

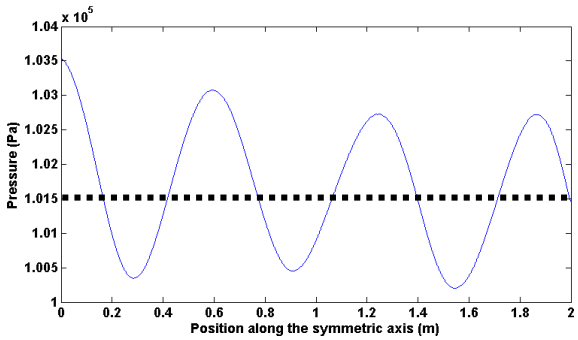

(b)

Figure 5 – Simulation results for corrugated channel alone. (a) Time series of velocity magnitude on the symmetry axis 20 mm upstream the corrugated channel outlet. (b) Spatial distribution of pressure along the symmetry axis of the corrugated channel at the last time step.

First calculations show the code ability to predict an aeroacoustics phenomenon though initial conditions only introduced aerodynamics aspect. We didn't impose acoustics that appeared naturally as a result of the simulation. As presented in figure 5, one can remark a 0.3s stabilization time for the calculation. Furthermore, for a uniform inlet velocity of 14ms^{-1}, the seventh mode is predominant. This inlet velocity corresponds to a mean bulk velocity estimated by PIV measurements for which the seventh mode was also highlighted. We can observe on figure 5 that respectively Neumann and Dirichlet acoustic boundary conditions are achieved at the inlet and the outlet of the corrugated channel. Both conditions are consistent with respect to the conditions imposed initially.

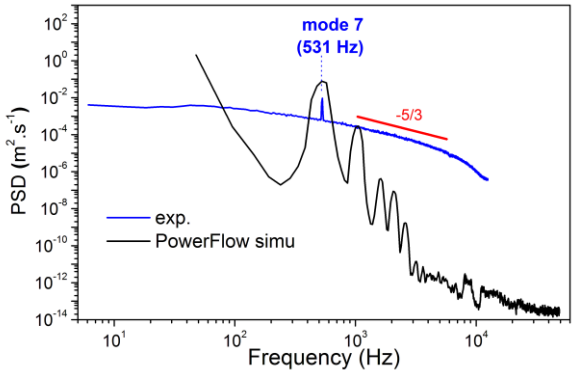

Figure 6 – Comparison of numerical (simulation results for corrugated channel alone) and experimental (hot-wire measurement) velocity spectral density.

Experimentally, the seventh mode has been obtained for a 17ms^{-1} velocity measured by hot-wire (positioned on the symmetry axis 20 mm upstream the corrugated channel outlet). The difference of aspect between the two spectra obtained numerically and experimentally is observed by comparing figures 6(a) and 6(b). It highlights that turbulence has not been correctly estimated by the code. This may result from a bad representation of the acoustics.

Further calculations were run considering larger calculation domains. This second set consists in four more calculations with varying inlet velocity for each calculation. The space and time averaged mean velocity in the corrugated pipe is here chosen as parameter for the four calculations: $U_0 = 4.5, 7.1, 8.3, 10.4\ ms^{-1}$. Choice of inlet velocity would not have been relevant since we are focusing on what's happening inside the pipe.

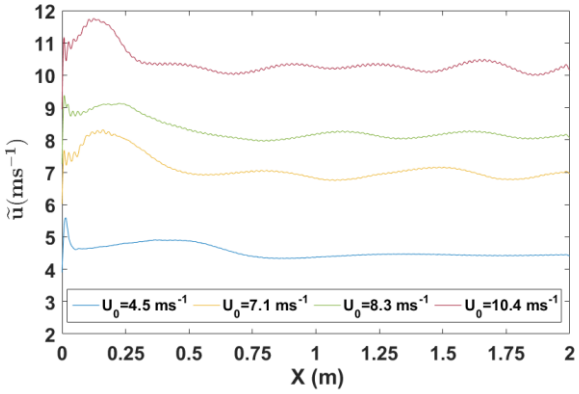

Figure 7 – Simulation results for corrugated channel + chambers. Time averaged mean velocity $\tilde{u}$ with respect to the position X along to the symmetry axis of the corrugated pipe for the set of calculations.

The time averaged mean velocity $\tilde{u}$ has been calculated for each position X along the symmetry axis (Figure 7). One can observe brutal acceleration on the upstream end (between 0 and 0.2m) of the corrugated pipe. This is due to a veina contracta phenomenon which can be explained by the important section reduction between the upstream chamber (390mm) and the corrugated pipe (20mm). As revealed on former paper [6], the veina contracta phenomenon appears to encourage the whistling on our experimental facility. As a result, the modelling of the flow outline on the first corrugations is one of our most concerning purpose.

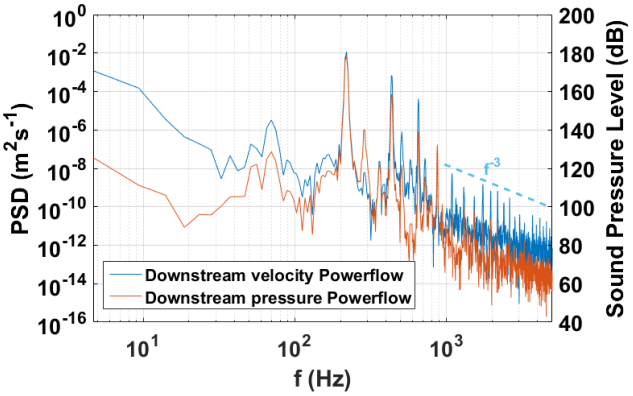

Figure 8 – Simulation results for corrugated channel + chambers. Velocity spectral density and sound pressure level for a mean velocity $U_0 = 7.1\ ms^{-1}$ at position X=1.9m, Y=0m.

Acoustic waves effectively travel in the corrugated channel as shown by spectral analysis of the density calculated by the LBM. One can calculate the velocity spectral density and the sound pressure level at 10mm upstream the corrugated pipe outlet (Figure 8). A located acoustic peak can be observed for each calculation (each U_0), as represented above.

The second set of calculations seems to better describe the acoustic phenomenon encountered experimentally than the first set (Figure 6 (a)). As well as the acoustic peaks appeared to be more located, turbulence seems to be better represented. Comparisons with traditional 2D turbulence modelling show a satisfactory concordance. At this location, the decay of the turbulence spectrum fits a f^{-3} slope, that is an expected result regarding the two-dimensional geometry [12].

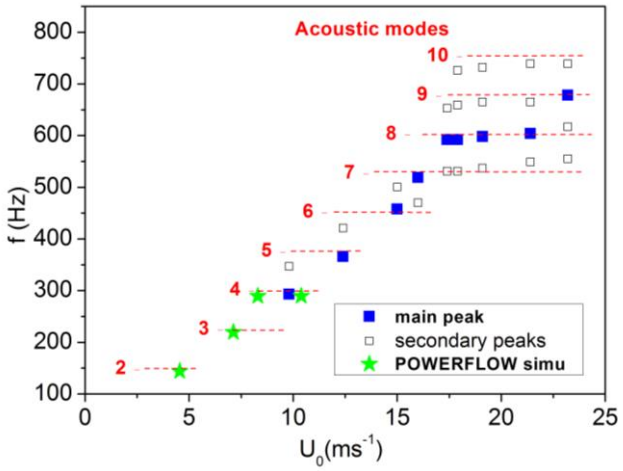

Figure 9 – Acoustic modes in the corrugated pipe. Experiments (in blue) and PowerFlow simulations (corrugated channel + chambers).

When the flow velocity increases, successive acoustic modes of the pipe appear (Figure 9). The frequencies of the acoustic modes observed on the flow simulations agree with the theoretical eigen frequencies of an open pipe with a corrected sound velocity c_{eff}: $f_n = \frac{nc_{eff}}{2\,L}$ with an acceptable relative error lower than 5%. A good agreement between experiment and simulation is obtained with the reference velocities [6].

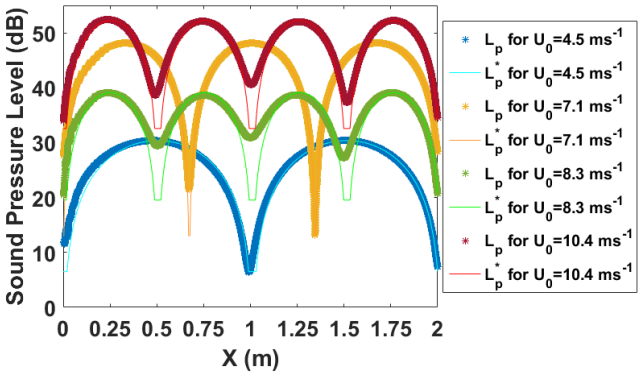

Figure 10 – Sound Pressure Level along the symmetry axis for each calculation. PowerFlow simulations (corrugated channel + chambers) and Eq. 7 fitting.

In figure 10, focus on sound pressure level along the symmetry axis is made for three acoustic modes associated to three reference velocities. Compared to the first calculations, the behavior appears to be very improved with respect to the result presented on the figure 6 since we can now observe Dirichlet boundary conditions at both ends of the corrugated pipe. Comparisons with theoretical modes show very good concordance:

$$L_p^* = 10\log\left(P_M^2 \sin\left(2n\pi\frac{x}{2(L+2\delta L)}\right)^2\right) \quad (7)$$

where P_M^2 is the amplitude measured, n indicates the mode under consideration. One obtains δL = 1 cm as the correction length of the channel, in line with the theoretical value [6]. The efficient speed of sound used for this modal identification, $c_{eff} = 299\,ms^{-1}$, has been calculated numerically by identifying modes with their corresponding acoustic frequencies and agrees with the experimental value [6].

CONCLUSION

We have adjusted a LBM simulation to our experimental facility. Two simulations have been held in order to do so. Since the modeling of the corrugated channel alone has presented various issues, we decided to improve our model by adding two chambers. Those adds have shown a real progress in the modeling of our experimental facility.

We have yet to simulate flow conditions with reference velocities higher than 10ms^{-1}. The objective is to catch the brutal acoustic amplification highlighted in the present experiment when the mean flow velocity is increased beyond a threshold velocity [6]. 3D simulations may provide a better estimation of sound pressure levels.

Once the simulation model is mastered and fits with the experimental results, a parametric study will be held. We may consider various parameters such as the corrugations shape and the pipe length.

ACKNOWLEDGEMENTS

The work presented herein is sponsored by TOTAL.

REFERENCES

[1] G. Nakiboglu, H.B.M. Manders, A. Hirschberg. Aeroacoustic power generated by a compact axisymmetric cavity: Prediction of self-sustained oscillation and influence of the depth, J. Fluid. Mech., 703, 163191 (2012).

[2] U.R. Kristiansen, G.A.Wiik. Experiments on sound generation in corrugated pipes with flow, J. Acoust. Soc. Am. 121, 13371444 (2007).

[3] B. Rajavel and M.G. Prasad, Acoustics of corrugated pipes: A review, Appl. Mech. Rev., 65: 050000/1-050000/24 (2013).

[4] M.S. Howe. Acoustics of fluid-structure interactions, Cambridge Monographs on Mechanics, Cambridge, University Press (1998).

[5] S.C. Morris. Shear-Layer Instabilities: Particle Image Velocimetry Measurements and Implications for Acoustics, Annu. Rev. Fluid Mech. 43, 529550 (2011).

[6] M. Amielh, F. Anselmet, Y. Jiang, U. Kristiansen, P.O. Mattei, D. Mazzoni, C. Pinhède. Aeroacoustic source analysis in a corrugated flow pipe using low-frequency mitigation, J. Turb., 15(10), 650676 (2014).

[7] J.M. Buick, C.A. Greated, D.M. Campbell, Lattice BGK simulation of sound waves. Europhys. Lett., 43(3), 235-240 (1998).

[8] H. Xu, P. Sagaut, Optimal low-dispersion low-dissipation LBM schemes for computational aeroacoustics, Journal of Comp. Phys. 230, 5353-5382 (2011).

[9] G. Galeron, D. Mazzoni, M. Amielh, P.O. Mattei, F. Anselmet, Experimental and numerical investigations of the aeroacoustic in a corrugated pipe flow, 4th International Conference on Turbulence and Interactions, Cargèse, France (2015).

[10] Y. Qian, D. D'Humieres, P. Lallemand, Lattice BGK Models for Navier-Stokes Equation. Europhys. Lett., 17 (6), 479-484 (1992).

[11] D.O. Martinez, W.H. Matthaeus, S. Chen, and D.C. Montgomery, Comparison of spectral method and lattice Boltzmann simulations of two-dimensional hydrodynamics, Phys. Fluids 6, 1285 (1994).

[12] P. Tabeling. Two-dimensional turbulence: a physicist approach, Phys. Rep. 362, 1-62 (2002).